





The diversified defocus profile of the near-work environment and myopia development

Kai Yip Choi¹ , Angela Yuen-ting Mok¹, Chi-wai Do¹ , Paul Hong Lee²  and Henry Ho-lung Chan¹ 

¹The Centre for Myopia Research, School of Optometry, The Hong Kong Polytechnic University, Kowloon, Hong Kong, and ²School of Nursing, The Hong Kong Polytechnic University, Kowloon, Hong Kong

Citation information: Choi KY, Mok AY-T, Do C-W, Lee PH, & Chan HH-L. The diversified defocus profile of the near-work environment and myopia development. *Ophthalmic Physiol Opt* 2020; 40: 463–471. <https://doi.org/10.1111/opo.12698>

Keywords: home size, living environment, myopia, near work

Correspondence: Henry H-L Chan
E-mail address: henryhl.chan@polyu.edu.hk

Received: 31 January 2020; Accepted: 4 May 2020; Published online: 9 June 2020

Author contributions: KYC: involved in all aspects of study conception and design, data acquisition, analysis and interpretation, and drafting and critically revising the manuscript; AYM: involved in data acquisition; CWD: involved in study conception and design; PHL: involved in data analysis; HHC: involved in study conception and design, and data interpretation.

Abstract

Purpose: To quantify the defocus characteristics in the near-work environment at home and investigate the relationship with subsequent myopia progression.

Methods: Fifty subjects (aged 7–12 years) were recruited and followed for 1 year. The home near-work environment (writing desk) was measured at a baseline home-visit using the Kinect-for-Windows to capture a 3-dimensional image. The depth values of the image were then converted into scene defocus with respect to the subject's viewpoint. The defocus characteristics were quantified as the dioptric volume (the total amount of net defocus, or DV) and standard deviation of the defocus values (SD_D). Information on home size, time spent outdoors, and in front of a desk were also obtained. Univariate correlation, and multivariate regression were used to assess the association between myopia progression, defocus characteristics, and other co-variables.

Results: The baseline spherical equivalent refraction (M) and refraction change over 1 year (ΔM) were -1.51 ± 2.02 D and -0.56 ± 0.45 D respectively. DV was not significantly correlated with ΔM (Spearman's $\rho = -0.25$, $p = 0.08$), while SD_D was negatively correlated to ΔM (Spearman's $\rho = -0.42$, $p = 0.003$). Although SD_D was not a significant predictor in multivariate analysis, the regional DV at 15° – 20° eccentricity was significant ($p = 0.001$). Home size ($F_{2,50} = 7.01$, $p = 0.002$) and time spent outdoors (Independent $t = -2.13$, $p = 0.04$) were also associated with ΔM , but not time spent in front of desk (Independent $t = 0.78$, $p = 0.44$).

Conclusion: The defocus profile in the home environment within the para-central field of view is associated with childhood refractive error development.

Introduction

Over the past decades, the prevalence of myopia has escalated in developed countries.¹ This rapid increase has been linked to environmental effects, which are critical for refractive error development.² In East and South-east Asian countries, the high prevalence of myopia has been attributed to the intense levels of near work during school age. Studies have quantified near work in terms of working distance,^{3,4} time span,^{5,6} type of near work,^{3,7} and weighted near work (i.e. dioptric hour).^{8,9} However, the relationship between near work and myopia remains controversial.¹⁰

Visual input at the peripheral retina has also been suggested to regulate eye growth. Animal studies have shown that despite absence of foveal integrity, peripheral visual signals could mediate central refractive development.^{11,12} Peripheral hyperopic and myopic defocus were found to cause myopic and hyperopic changes, respectively.¹² This phenomenon is reflected in the success of myopia control in terms of manipulating defocus over most of the retina using orthokeratology,¹³ multifocal contact lenses,¹⁴ and defocus-incorporated spectacle lenses.¹⁵ However, it remains controversial whether the myopia control effect emanates from the peripheral myopic defocus

induced by these devices,¹⁶ as several studies showed that initial peripheral refractive errors in children were not associated with the incidence or onset of myopia.^{17,18} In addition, other designs of myopia control intervention targeting reduction of peripheral hyperopia, failed to effectively control refractive development in children.¹⁹ Although it is generally accepted that the peripheral retina plays a role in ocular growth, the relationship between peripheral refractive error and myopia development still needs further investigation.

In daily life, human eyes are exposed simultaneously to myopic and hyperopic defocus from the environment.²⁰ Based on the simultaneous defocus concept, Flitcroft simulated human visual scenes using customised computer software.²¹ In this simulation, outdoor scenes have a more evenly-distributed dioptric profile, while indoor scenes (within an office) have an uneven dioptric profile. The distribution of the defocus is even more varied when indoor object distance is closer. The uneven distribution of peripheral defocus from the indoor environment was suggested as a myopia risk factor for children, especially those who spent less time outdoors, to have a higher incidence and prevalence of myopia.^{21,22} In a previous study, it was reported that small home size in Hong Kong was associated with more myopia and longer axial length.²³ The reason for this increased risk was suggested to be the peripheral hyperopic defocus due to the close surroundings in small homes. However, it is still unknown whether certain home environment characteristics, for example, reading desk scenes, other than home size, could contribute to children's refractive development.

In Hong Kong and elsewhere in East-Asia, children spend many hours in near work at home to complete their heavy load of school work.^{24,25} It is important to understand how the home-working environment, especially for near tasks, affects their refractive errors. Myopia studies investigating near tasks have focused mainly on the type of visual task, while the details of the visual scene, for example, the dioptric profile, received little attention. With the emergence of depth sensing technology,^{26,27} it is possible to obtain more information (e.g. depths across the visual field) from a scene with a handy device.^{28,29} In the current study, it was aimed to quantify the amount of relative scene defocus in a near-work environment, and investigate the relationship between such environments and juvenile refractive development.

Methods

Subjects and ocular data

Fifty-nine healthy Chinese subjects aged between 7 and 12 years were recruited in the Optometry Clinic of The Hong Kong Polytechnic University to participate in the

study from December 2016 to October 2017. Six subjects were excluded because they started orthokeratology ($n = 1$), had a major home renovation ($n = 1$), or were lost to follow-up ($n = 4$) within the study period. An additional three subjects were excluded because they had a glass-surfaced working desk, creating specular reflection, preventing measurement of the dioptric profile. Informed consent and simple written assent were obtained from the parent and the subject, respectively. The study protocols were approved by the Human Subjects Ethics Subcommittee of The Hong Kong Polytechnic University and all procedures followed the tenets of the Declaration of Helsinki. Subjects attended an initial eye examination in the clinic and a second follow-up a year later. Cycloplegic refraction, using an open-field autorefractor (NVision K5001, <http://www.shin-nippon.jp/products/nvk5001/>), was measured 30 min after instilling two drops of 1% cyclopentolate five minutes apart. Five measurements were taken and the value was transposed into spherical equivalent refraction (M) using the following equation:

$$M = S + \frac{C}{2},$$

where S is the spherical error and C is the cylindrical error.

The change in M (ΔM) in the right eye after 1 year was analysed.

Home visit and visual scene measurement

Each subject's home was visited to capture the daily visual scene before the baseline eye examination. As children in Hong Kong spend hours on school work,^{24,25} their reading desk (for near tasks) was chosen as the target visual scene. The daily time in front of the desk, as well as weekly time outdoors, were reported by the subject and confirmed by the parent/guardian. Subjects were asked to perform some near work sitting in their usual position at the desk, which was confirmed by their parent/guardian. The desk was presented in its usual format, with the subject's own home-work exercise book in place. The distance from the visual target (a book) to the eye position was measured using a metric tape. The photograph of home scene was shown to the parent/guardian at the 1-year follow up visit to confirm there was no major change of furniture position.

To obtain the information of the visual scene, Kinect-for-Windows v2 (Hardware discontinued in 2017, software development kit available on <https://www.microsoft.com/en-hk/download/details.aspx?id=44561>) was used to capture the scene depth in the first visit.^{26,27} It consists of an infra-red emitter and an infra-red camera, which allow the device to capture the scene depth by calculating the time of flight of the infra-red light ray. Before the measurement, subjects were first asked to take up their usual working

posture, which was confirmed by their parent/guardian. Because of the working range of the device (0.5 m–4.5 m), the Kinect was set 50 cm behind the subject's eye position. The Kinect was directed to point at the visual target (e.g. a book) and aligned with the subject's line of sight on a monopod to maintain stability. Subjects were then asked to leave the scene and the scene depth was captured for at least 5 s at a frequency of 1 Hz, i.e. a total of at least five depth images were obtained (Figure 1). The Kinect depth images, which were superimposed to obtain the average values, consisted of 512×434 pixels carrying a distance value corresponding to the points in the scene from the device.

Data processing and analysis

As the Kinect was placed behind the subject, the values were corrected by calibrating the central pixel value according to the actual viewing distance measured by the metric

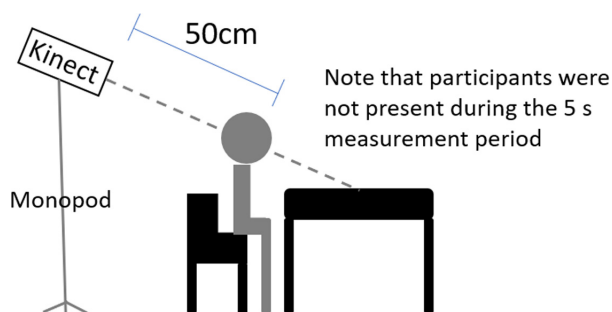


Figure 1. Schematic diagram of the measurement setup.

tape. The depth values were inverted to dioptres, and then calibrated with respect to the centre of the visual target, e.g. a book on the desktop, which was set as zero. Hence, the points, which were further away than the visual target, would be of negative dioptic value (myopic defocus), while those closer than the visual target would be of positive dioptic value (hyperopic defocus). Finally, the visual scene was reconstructed using the dioptic depth values across vertical and horizontal dimensions, i.e. a 3-dimensional dioptic space,³⁰ with respect to the subject's viewpoint. If there was any window within the measured field, this part of the scene would be regarded as no vergence (i.e. distant with respect to the central visual target). One of the limitations of the current study was the lack of eye fixation data, in which the scene defocus could not be mapped with the retinal defocus. Another limitation was the lack of continuity of data acquisition, in which baseline data was obtained.

To represent the overall dioptic power of the visual scene, the dioptic volume (DV) of the scene was defined as the approximate double integrals computed by *trapz* function in MATLAB (www.mathworks.com) over the central 30° field of view (i.e. dioptre \times degree², or D°°). The DV was calculated based on both linear (assuming the positive and negative powers cancelled each other out) and non-linear (assuming myopic defocus was twice potent of hyperopic defocus, i.e. DV_{2M})²⁰ relationships. Central 30° field of view was chosen because this could accommodate all subjects with different working distances within the device's working angle of view. In simple terms, the dioptic volume represented the total amount of net defocus generated from the scene with respect to the central visual

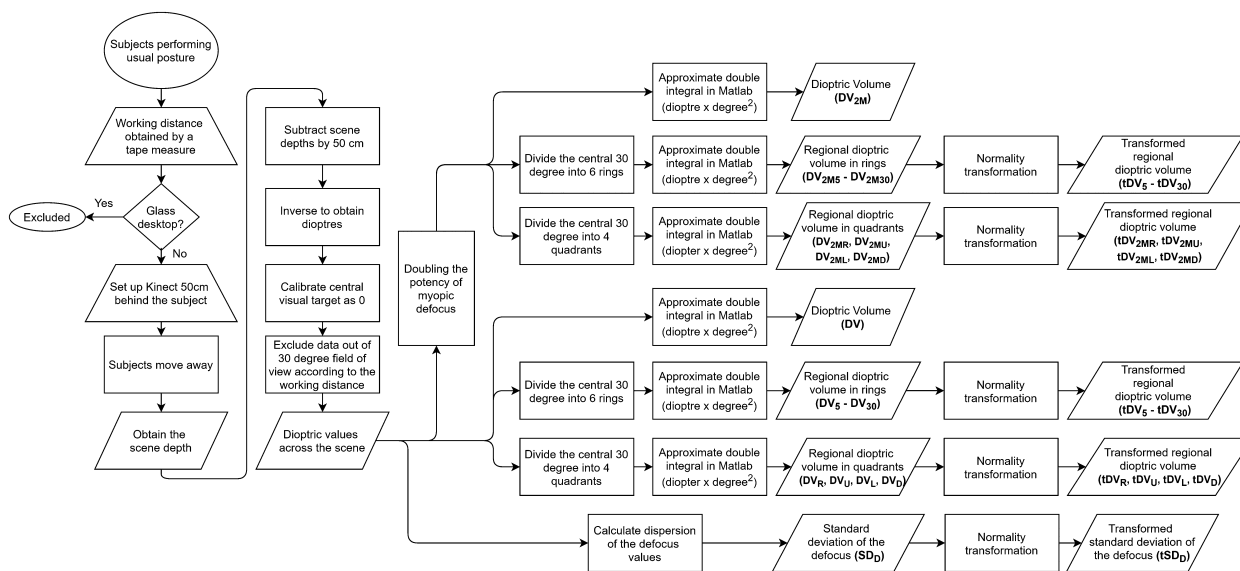


Figure 2. Flow chart for defocus data acquisition and processing.

target. In addition, to assess the overall dispersion of the scene dioptric defocus, the standard deviation of the scene defocus (SD_D) was also calculated. A flow-chart summarizing the procedures is shown in Figure 2. The partial correlation between DV and ΔM , and between SD_D and ΔM were calculated using Spearman's test, with baseline M as the confounding factor.

To assess the regional effect, the central 30° field of view was divided into six rings of 5° interval and four quadrants (right, up, left, and down) respectively (Figure 3). The DV was calculated in each ring and quadrant to evaluate the effect of eccentricity and location of the scene respectively. To simplify the statistics, the regional DVs were transformed to achieve normality using a two-step transformation³¹ (Before transformation: K-S tests > 0.18 , $p < 0.001$;

after transformation: K-S tests < 0.04 , $p > 0.20$). The correlation between transformed dioptric volume in each ring (i.e. tDV_5 to tDV_{30}) and ΔM , and between quadrant (i.e. tDV_R , tDV_U , tDV_L , and tDV_D) and ΔM were individually calculated using Spearman's test, and then entered into multiple linear regression models, as well as other factors, including age, baseline M , time spent in front of desk, time spent outdoors, working distance, parental myopia (by self-reporting), home size, and transformed SD_D (tSD_D), to predict the 1-year ΔM of the subject. The stepwise removal method was further used to cater for our small sample size in the regression models, which was to eliminate insignificant variables starting from the one with the highest p value, until the p values of all remaining variables were below 0.05.

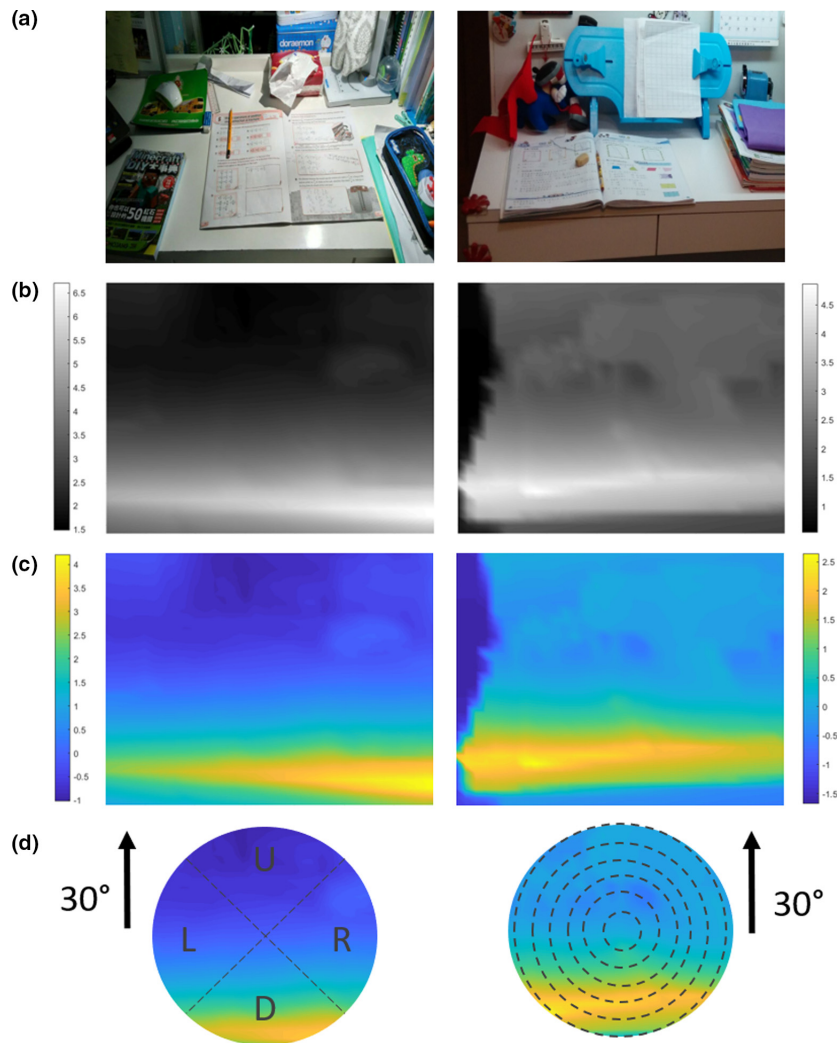


Figure 3. Scene demonstration of subjects' desks. (a) Coloured picture. (b) Dioptic (inversed distance) map. (c) Scene defocus map after calibration. (d) Analysis region of central 30° . This region was divided into six rings and four quadrants respectively for secondary analysis. Positive defocus indicates hyperopic while negative defocus indicates myopic defocus. Colour scale in dioptres.

It was previously reported that home size was associated with the childhood refractive error of Hong Kong children. In the current study, the relationship between home size and ΔM , as well as the DV and SD_D were investigated. Subjects were sequenced according to their home sizes and were categorised into three groups: Small ($N = 16$, Range 297–500 ft²/27.6 – 46.5 m²), Medium ($N = 17$, Range 503–602 ft²/46.7–5.9 m²), and Large ($N = 17$, Range 614–1400 ft²/57.0–130.1 m²). One-way analysis of variance (or Kruskal-Wallis test) was used to compare the ΔM , DV, and SD_D , with Bonferroni post-hoc test, among the three home size groups. The ΔM was also compared among parental myopia using one-way analysis of variance with Bonferroni post-hoc test. In addition, the daily time spent in front of the desk and weekly time spent outdoor (transportation excluded) were classified as Low [<2 h/day²⁴ and <2 h/week (median), respectively] and High (≥ 2 h/day and ≥ 2 h/week) respectively, with which the ΔM were then compared using separate independent *t*-tests. Only the data from the right eye was analysed. Significance level was set at 0.05 and all tests were performed with SPSS Statistics V22.0 software (<https://www.ibm.com/analytics/spss-statistics-software>).

Results

The subjects ($n = 50$) in the study were aged 9.3 ± 1.2 years (Mean \pm S.D.) and had a baseline refraction of -1.51 ± 2.02 D. The ΔM was -0.56 ± 0.45 D over 1 year. The median daily time subjects spent in front of the desk was 2 h/day (IQR 1.0–3.0 h/day, Range 0.5–5.0 h/day), with an average working distance of 29.7 ± 6.0 cm, while the median weekly time spent outdoor was 2 h/week (IQR 1.0–4.5 h/week, Range 1.0–20.0 h/week). With

respect to the scene defocus parameters, the median DV and DV_{2M} over the central 30° were 1.16 D° (IQR 0.46–3.82 D°, Range -0.48 –8.43 D°) and 0.86 D° (IQR 0.27 to 3.56 D°, Range -1.36 to 8.24 D°), while the median SD_D over the central 30° was 0.49 D° (IQR 0.31–0.69 D°, Range 0.08–2.29 D°).

The working distance of the subjects was not related to the ΔM (Pearson’s $R = 0.21$, $p = 0.15$), but was negatively correlated with DV (Spearman’s $\rho = -0.60$, $p < 0.001$) and SD_D (Spearman’s $\rho = -0.67$, $p < 0.001$) respectively. Thus, the shorter the working distance, the more positive and dispersed the overall scene defocus. For the partial correlation controlling for the baseline M, DV (Spearman’s $\rho = -0.25$, $p = 0.08$) and DV_{2M} (Spearman’s $\rho = -0.21$, $p = 0.16$) were not related to ΔM , while SD_D was negatively correlated to ΔM (Spearman’s $\rho = -0.42$, $p = 0.003$), i.e. subjects with faster myopia progression had a more dispersed baseline scene defocus.

Among the regional defocus, DV_{20} was significant correlated with ΔM (Spearman’s $\rho = -0.32$, $p = 0.02$) but no quadrant DV nor DV_{2M} was correlated. Table 1 shows the statistical results of other correlations. Multiple regression analyses revealed that only age, baseline M, and tDV_{20} were significantly associated with ΔM in the regression models. Tables S1–S4 list the detailed statistical analyses of individual variable. The results from the step-wise regression models showed that older children and those having more hyperopic baseline M had significantly slower myopia progression. On the other hand, more hyperopic para-central defocus at 15°–20° (i.e. tDV_{20} and tDV_{2M20}) and left quadrant (i.e. tDV_L and tDV_{2ML}) from the scene were associated with faster myopia progression. The coefficients and statistics of the significant variables are listed in Table 2.

Table 1. Correlation between regional defocus and refractive change over 1 year

	DV ₅	DV ₁₀	DV ₁₅	DV ₂₀	DV ₂₅	DV ₃₀
Spearman’s ρ	-0.12	-0.12	-0.23	-0.32†	-0.13	0.04
<i>p</i> Value	0.42	0.40	0.11	0.02	0.37	0.78
	DV _R		DV _U		DV _L	
Spearman’s ρ	-0.18		0.27		-0.22	
<i>p</i> value	0.21		0.06		0.12	
	DV _{2M5}	DV _{2M10}	DV _{2M15}	DV _{2M20}	DV _{2M25}	DV _{2M30}
Spearman’s ρ	-0.15	-0.08	-0.23	-0.22	-0.07	0.11
<i>p</i> value	0.30	0.56	0.12	0.12	0.63	0.47
	DV _{2MR}		DV _{2MU}		DV _{2ML}	
Spearman’s ρ	-0.16		0.26		-0.19	
<i>p</i> value	0.27		0.06		0.20	

DV, dioptic volume; D, Down; L, Left; R, Right; U, Up. 2M indicates 2× myopic defocus potency.

†Indicates a significance level of < 0.05 .

Table 2. Stepwise multiple regression on refractive change over 1 year

	Raw B value	95% CI	Standardised B value	p Value	VIF
1× myopic defocus potency ring analysis: Adjusted $R^2 = 0.32$, $F_{3,50} = 8.63$, $p < 0.001$					
Age	0.12	0.03 to 0.29	0.31	0.01	1.02
Baseline M	0.05	0.01 to 0.11	0.24	0.05	1.01
tDV ₂₀	-0.18	-0.28 to -0.08	-0.43	0.001	1.03
1× myopic defocus potency quadrant analysis: Adjusted $R^2 = 0.18$, $F_{3,50} = 4.58$, $p = 0.01$					
One myopic parent	-0.38	-0.68 to -0.07	-0.34	0.02	1.10
tDV _U	0.14	0.02 to 0.26	0.31	0.03	1.10
tDV _L	-0.17	-0.28 to -0.05	-0.40	0.01	1.11
2× myopic defocus potency ring analysis: Adjusted $R^2 = 0.31$, $F_{3,50} = 8.18$, $p < 0.001$					
Age	0.12	0.03 to 0.21	0.32	0.01	1.02
Baseline M	0.06	0.01 to 0.12	0.28	0.03	1.04
tDV _{2M20}	-0.18	-0.28 to -0.07	-0.42	0.001	1.05
2× myopic defocus potency quadrant analysis: Adjusted $R^2 = 0.16$, $F_{4,50} = 4.09$, $p = 0.01$					
Medium home size	0.26	0.01 to 0.51	0.28	0.04	1.04
High time spent outdoors	0.27	0.04 to 0.50	0.31	0.02	1.04
tDV _{2ML}	-0.28	-0.58 to -0.00	-0.26	0.05	1.05
tSD _D	-0.13	-0.25 to 0.02	-0.31	0.02	1.08

tDV, transformed dioptic volume; tSD_D, transformed standard deviation of the defocus; R, Right; U, Up; L, Left; D, Down. 2M indicates 2× myopic defocus potency.

The univariate analyses are listed in *Table 3*. Home size was associated with ΔM (One-way ANOVA, $F_{2,50} = 7.01$, $p = 0.002$), but not with DV (Kruskal-Wallis test, $\chi^2_{2,50} = 0.40$, $p = 0.82$), DV_{2M} (Kruskal-Wallis test, $\chi^2_{2,50} = 0.44$, $p = 0.80$), or SD_D (Kruskal-Wallis test, $\chi^2_{2,50} = 3.81$, $p = 0.15$). In post-hoc tests, children living in a Small-sized home had greater myopia progression than those in a Medium-sized (Bonferroni post-hoc test, $p = 0.02$) and Large-sized home (Bonferroni post-hoc test, $p = 0.003$). No significant association was found between Medium- and Large-sized homes (Bonferroni post-hoc test,

$p > 0.99$). Parental myopia was not significantly associated with ΔM (One-way ANOVA, $F_{2,50} = 2.44$, $p = 0.10$). There was no significant difference between the Low and High groups (Independent $t = 0.78$, $p = 0.44$) for daily time spent in front of their desk. With respect to the weekly time spent outdoors, the Low group progressed significantly faster than the High group (Independent $t = -2.13$, $p = 0.04$), but, neither the correlation between time spent outdoors and scene defocus (DV: Spearman's $\rho = -0.24$, $p = 0.10$; SD_D: Spearman's $\rho = -0.15$, $p = 0.30$) nor the correlation between daily time spent in front of desk and scene defocus (DV: Spearman's $\rho = 0.13$, $p = 0.36$; SD_D: Spearman's $\rho = 0.15$, $p = 0.29$) reached significance.

Table 3. Univariate analyses on myopia progression over 1 year

	N	ΔM (Mean \pm S.D.)
Total	50	-0.56 \pm 0.45 D
Home size		
Small home	16	-0.87 \pm 0.52 D†
Medium home	17	-0.46 \pm 0.32 D†
Large home	17	-0.38 \pm 0.35 D†
Parental myopia		
No myopic parent	6	-0.23 \pm 0.43 D
One myopic parent	21	-0.67 \pm 0.52 D
Two myopic parents	23	-0.55 \pm 0.35 D
Time spent in front of desk		
Low (<2.0 h daily)	21	-0.50 \pm 0.47 D
High (\geq 2.0 h daily)	29	-0.61 \pm 0.43 D
Time spent outdoors		
Low (<2.0 h weekly)	24	-0.70 \pm 0.47 D§
High (\geq 2.0 h weekly)	26	-0.44 \pm 0.40 D§

†‡ Significant difference in Bonferroni post-hoc test.

§ Significant difference in independent t -test.

Discussion

The current study revealed an association between children's home-working environment and their subsequent refractive development. Specifically, the defocus profile from the scene, in terms of the dispersion of defocus distribution and para-central regional defocus, was associated with the myopic change in refractive error in a year. As reported previously, small home size was not only associated with more myopic refractive error, but also a risk factor for faster myopic change.

Findings for adverse effects of near work on childhood refractive development are controversial.¹⁰ In the current study, a novel quantification of a near work environment was devised. Garcia and co-workers described their measurements to capture the defocus map using an older version of Kinect (v1) and an eye tracker²⁹ by overlapping the

acquired frames from both devices over five minutes. Unlike the computer working desk in their study, the ‘in-focus’ area of a child’s writing/reading desk did not show a maximum (Figure 4) because the desk surface was inclined with respect to the eyes. Instead, most of the area of view incorporated a range of negative defocus. However, the calculated DVs, which is the total amount of net defocus of the central 30° field, for most subjects were positive, because the magnitude of the positive defocus was generally greater than that of negative defocus. Figure 4 shows the representative distributions (quartiles) regarding DV and SD_D, which is the dispersion of scene defocus value within the central 30°.

These findings suggest a moderate correlation between peripheral defocus dispersion and myopia progression. Unlike an outdoor scene, in which peripheral defocus distribution is more uniform, an indoor scene consists of a more varied defocus profile, creating a rapid change in

peripheral retinal defocus when the fixation is changed. Such rapid change has been suggested to cause a failure in emmetropization as the temporal integration of the retinal signals is interrupted,^{21,22} in which this non-linear temporal integration was demonstrated in studies performed in both guinea pigs and monkeys.^{32,33} With respect to spatial integration, myopic defocus demonstrated approximately twice the potency of hyperopic defocus when simultaneously presented in chicks.²⁰ In the current study, this doubled myopic potency assumption could not better explain the relationship between scene defocus and myopic progression, which may be due to the difference in species as the myopic potency appeared less prominent in mammals.³⁴ In addition, as in an earlier study conducted by our group, a smaller home was associated with more myopic refractive error.²³ We speculated a smaller home would create more surrounding hyperopic defocus, as the constricted environment would

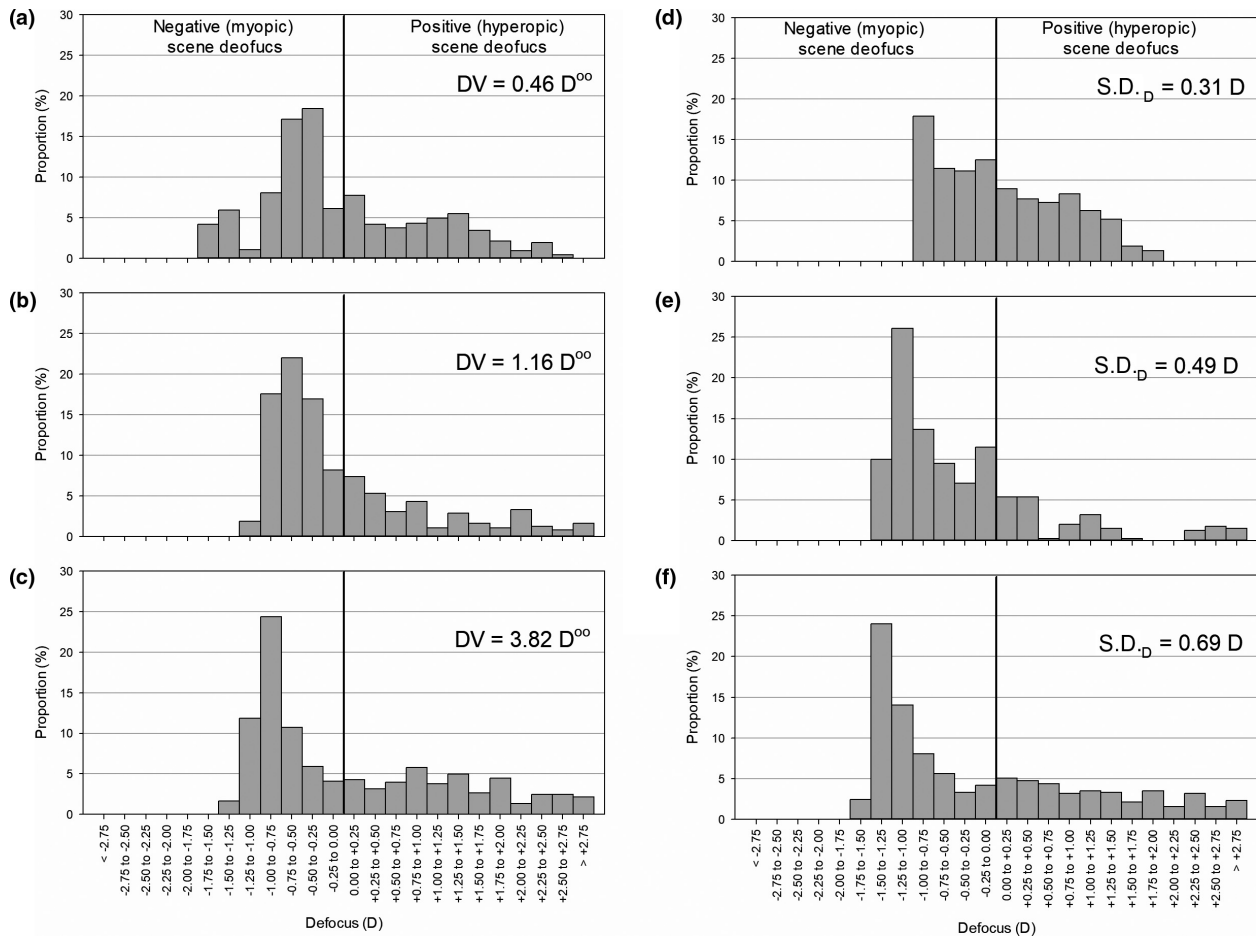


Figure 4. Scene defocus distribution of central 30° from representative subjects – Subject a: The 1st quartile of dioptric volume (DV); Subject b: The 2nd quartile of DV; Subject c: The 3rd quartile of DV; Subject d: The 1st quartile of standard deviation of the scene defocus (SD_D); Subject e: The 2nd quartile of SD_D; Subject f: The 3rd quartile of SD_D. The DV represented the total amount of net defocus, while the SD_D represented the dispersion of scene defocus value within the central 30°.

block the view of distant objects and/or have more close objects.

In contrast, the total amount of net defocus within the central 30° field (i.e. DV and DV_{2M}) was not associated with refractive error development. Instead, the amount of net defocus across 15°–20° eccentricity had a modest, but significant correlation with the change in refractive error as well as the multiple linear regression analysis controlled for other covariates. Unfortunately, it was not possible to match the scene defocus with the subjects' fixation to generate the retinal defocus map as illustrated by Garcia *et al.*³⁵ However, the para-central retina has been reported to have higher defocus sensitivity in electroretinography studies.^{36,37} If the scene eccentricity is matched with the retinal eccentricity, the positions of the closely surrounding objects near the central visual target is likely to manipulate the peripheral retinal signal in control of the emmetropization process. However, quadrant analysis did not show any conclusive association with myopia progression. Among the four quadrants, the left quadrant was significantly associated with DV in multivariate analyses, but not univariate analyses. A possible explanation could be the writing habit due to the dominance of right laterality, but further study is necessary to determine if this is the case.

To our knowledge, the current study is the first to investigate home environmental defocus in relation to children's refractive error development. Yet, there are several limitations preventing a comprehensive interpretation of the results. Firstly, the defocus profile measurement was performed at a single time point instead of longitudinally incorporating observation of changes in the environment, meaning that only the subsequent refractive change throughout the year with the baseline environmental defocus could be observed. Secondly, the DV was calculated as a net defocus over the 3-dimensional space, assuming the positive and negative defocus would equally cancel each other out. Finally, as the subjects were required to move away during the measurement, such a move would ignore the defocus created by the subjects' own body parts, e.g. arms placed on the desk. In future studies, handy smartphones with duo, or even trio-camera could be used to gather longitudinal data at a larger scale. In addition, eye trackers could have been incorporated into the measurement to map the environmental defocus onto the retinal defocus,³⁵ as well as to investigate the defocus temporal integration,^{32,33,38} to evaluate myopia development.

Conclusion

The defocus profile in the home environment, especially within the para-central field of view, is associated with childhood refractive error development and is likely a potential myopia risk factor.

Acknowledgements

The authors acknowledge Dr Maureen Boost for providing advice in the preparation of the manuscript. This study was supported by General Research Fund from the Research Grants Council of the Hong Kong Special Administrative Region, China (PolyU 151001/17M) and Internal Research Grants, The Hong Kong Polytechnic University (Z0GF).

Conflict of interest

The authors report no conflicts of interest and have no proprietary interest in any of the materials mentioned in this article.

References

1. Holden BA, Fricke TR, Wilson DA *et al.* Global prevalence of myopia and high myopia and temporal trends from 2000 through 2050. *Ophthalmology* 2016; 123: 1036–1042.
2. Morgan IG, Ohno-Matsui K & Saw SM. Myopia. *Lancet* 2012; 379: 1739–1748.
3. Ip JM, Saw S-M, Rose KA *et al.* Role of near work in myopia: findings in a sample of Australian school children. *Invest Ophthalmol Vis Sci* 2008; 49: 2903–2910.
4. Li S-M, Li S-Y, Kang M-T *et al.* Near work related parameters and myopia in Chinese children: the Anyang Childhood Eye Study. *PLoS One* 2015; 10: e0134514.
5. Mutti DO, Mitchell GL, Moeschberger ML, Jones LA & Zadnik K. Parental myopia, near work, school achievement, and children's refractive error. *Invest Ophthalmol Vis Sci* 2002; 43: 3633–3640.
6. Saxena R, Vashist P, Tandon R *et al.* Prevalence of myopia and its risk factors in urban school children in Delhi: the North India Myopia Study (NIM Study). *PLoS One* 2015; 10: e0117349.
7. Saw SM, Nieto FJ, Katz J, Schein OD, Levy B & Chew SJ. Factors related to the progression of myopia in Singaporean children. *Optom Vis Sci* 2000; 77: 549–554.
8. Saw SM, Chua WH, Hong CY *et al.* Nearwork in early-onset myopia. *Invest Ophthalmol Vis Sci* 2002; 43: 332–339.
9. Saw SM, Zhang MZ, Hong RZ, Fu ZF, Pang MH & Tan DT. Near-work activity, night-lights, and myopia in the Singapore-China study. *Arch Ophthalmol* 2002; 120: 620–627.
10. Huang HM, Chang DS & Wu PC. The association between near work activities and myopia in children-A systematic review and meta-analysis. *PLoS One* 2015; 10: e0140419.
11. Smith EL 3rd, Kee CS, Ramamirtham R, Qiao-Grider Y & Hung LF. Peripheral vision can influence eye growth and refractive development in infant monkeys. *Invest Ophthalmol Vis Sci* 2005; 46: 3965–3972.
12. Smith EL, Hung L-F & Huang J. Relative peripheral hyperopic defocus alters central refractive development in infant monkeys. *Vision Res* 2009; 49: 2386–2392.

13. Cho P & Cheung SW. Retardation of Myopia in Orthokeratology (ROMIO) study: a 2-year randomized clinical trial. *Invest Ophthalmol Vis Sci* 2012; 53: 7077–7085.
14. Lam CS, Tang WC, Tse DY, Tang YY & To CH. Defocus Incorporated Soft Contact (DISC) lens slows myopia progression in Hong Kong Chinese schoolchildren: a 2-year randomised clinical trial. *Br J Ophthalmol* 2014; 98: 40–45.
15. Lam CSY, Tang WC, Tse DY *et al.* Defocus Incorporated Multiple Segments (DIMS) spectacle lenses slow myopia progression: a 2-year randomised clinical trial. *Br J Ophthalmol* 2020; 104: 363–368.
16. Smith EL, Campbell MC & Irving E. Does peripheral retinal input explain the promising myopia control effects of corneal reshaping therapy (CRT or ortho-K) & multifocal soft contact lenses? *Ophthalmic Physiol Opt* 2013; 33: 379–384.
17. Mutti DO, Sinnott LT, Mitchell GL *et al.* Relative peripheral refractive error and the risk of onset and progression of myopia in children. *Invest Ophthalmol Vis Sci* 2011; 52: 199–205.
18. Atchison DA, Li S-M, Li H *et al.* Relative peripheral hyperopia does not predict development and progression of myopia in children. *Invest Ophthalmol Vis Sci* 2015; 56: 6162–6170.
19. Sankaridurg P, Donovan L, Varnas S *et al.* Spectacle lenses designed to reduce progression of myopia: 12-month results. *Optom Vis Sci* 2010; 87: 631–641.
20. Tse DY & To CH. Graded competing regional myopic and hyperopic defocus produce summated emmetropization set points in chick. *Invest Ophthalmol Vis Sci* 2011; 52: 8056–8062.
21. Flitcroft D. The complex interactions of retinal, optical and environmental factors in myopia aetiology. *Prog Retin Eye Res* 2012; 31: 622–660.
22. Charman WN. Keeping the world in focus: how might this be achieved? *Optom Vis Sci* 2011; 88: 373–376.
23. Choi KY, Yu WY, Lam CHI *et al.* Childhood exposure to constricted living space: a possible environmental threat for myopia development. *Ophthalmic Physiol Opt* 2017; 37: 568–575.
24. 香港學童餘暇生活調查 2014. *Leisure Activities of Hong Kong Schoolchildren 2014*. Hong Kong Professional Teachers' Union, Research E: Hong Kong, 2015.
25. 2017-18學年小學生學習狀況調查報告 . *2017-18 Report on Primary Schoolchildren Learning*. Hong Kong Professional Teachers' Union, Research E: Hong Kong, 2018.
26. Khoshelham K & Elberink SO. Accuracy and resolution of kinect depth data for indoor mapping applications. *Sensors* 2012; 12: 1437–1454.
27. Gonzalez-Jorge H, Rodríguez-González P, Martínez-Sánchez J *et al.* Metrological comparison between Kinect I and Kinect II sensors. *Measurement* 2015; 70: 21–26.
28. Sprague WW, Cooper EA, Reissier S, Yellapragada B & Banks MS. The natural statistics of blur. *J Vis* 2016; 16: 23–23.
29. Garcia MG, Ohlendorf A, Schaeffel F & Wahl S. Dioptric defocus maps across the visual field for different indoor environments. *Biomed Opt Express* 2018; 9: 347–359.
30. Flitcroft D, editor. *Dioptric space: extending the concepts of defocus to three dimensions*. ARVO Annual Meeting; Fort Lauderdale, Florida, USA, 2006.
31. Templeton GF. A two-step approach for transforming continuous variables to normal: implications and recommendations for IS research. *Commun Assoc Inform Syst* 2011; 28: 4.
32. Leotta AJ, Bowrey HE, Zeng G & McFadden SA. Temporal properties of the myopic response to defocus in the guinea pig. *Ophthalmic Physiol Opt* 2013; 33: 227–244.
33. Benavente-Perez A, Nour A & Troilo D. Short interruptions of imposed hyperopic defocus earlier in treatment are more effective at preventing myopia development. *Sci Rep* 2019; 9: 11459.
34. McFadden SA, Tse DY, Bowrey HE *et al.* Integration of defocus by dual power Fresnel lenses inhibits myopia in the mammalian eye. *Invest Ophthalmol Vis Sci* 2014; 55: 908–917.
35. Garcia Garcia M, Pusti D, Wahl S & Ohlendorf A. A global approach to describe retinal defocus patterns. *PLoS One* 2019; 14: e0213574.
36. Ho WC, Wong OY, Chan YC, Wong SW, Kee CS & Chan HH. Sign-dependent changes in retinal electrical activity with positive and negative defocus in the human eye. *Vision Res* 2012; 52: 47–53.
37. Chin MP, Chu PH, Cheong AM & Chan HH. Human electroretinal responses to grating patterns and defocus changes by global flash multifocal electroretinogram. *PLoS One* 2015; 10: e0123480.
38. Leung TW, Flitcroft DI, Wallman J *et al.* A novel instrument for logging nearwork distance. *Ophthalmic Physiol Opt* 2011; 31: 137–144.

Supporting Information

Additional Supporting Information may be found in the online version of this article:

Table S1. Multiple regression with all variables on refractive change over 1 year by ring analysis.

Table S2. Multiple regression with all variables on refractive change over 1 year by quadrant analysis.

Table S3. Multiple regression with all variables with doubled myopic defocus potency on refractive change over 1 year by ring analysis.

Table S4. Multiple regression with all variables with doubled myopic defocus potency on refractive change over 1 year by quadrant analysis.

Table S5. Descriptive statistics of the regional dioptric volume.